Nearfield Beamforming Using Radial Reciprocity

Rodney A. Kennedy, *Member, IEEE*, Darren B. Ward, and Thushara D. Abhayapala, *Student Member, IEEE*

***Abstract*—We establish the asymptotic equivalence, up to complex conjugation, of two problems: 1) determining the nearfield performance of a farfield beampattern specification and 2) determining the equivalent farfield beampattern corresponding to a nearfield beampattern specification. Using this reciprocity relationship, we develop a computationally simple procedure to design a beamforming array to achieve a desired nearfield beampattern response. The superiority of this approach to existing methods, both in ease of design implementation and performance obtained, is analyzed and then illustrated by a design example.**

***Index Terms*— Array processing, broadband beamforming, nearfield beamforming.**

I. Introduction

THE MAJORITY of array processing literature deals with the case in which the source is assumed to be in the farfield of the array, and hence, the received wavefront from a single point source is planar. This assumption significantly simplifies the beamformer design problem. The common rule of thumb is that farfield operation can be assumed for sources at a distance of

$$r = 2L^2/\lambda$$

where

- r radial distance from an arbitrary array origin;
- L largest array dimension;
- λ operating wavelength [1].

However, in many practical situations,[1] the source is well within this distance and using the farfield assumption to design the beamformer results in severe degradation in the beampattern. Despite this, nearfield beamforming is a problem that has been largely ignored in the signal processing literature.

One common design method for nearfield beamforming is *nearfield compensation* (e.g., [4]) in which a delay correction is used on each sensor to account for the nearfield spherical wavefronts. This method depends on the array geometry and takes its simplest form when the sensors are colinear. Even with the simplest array geometries, designs based on nearfield compensation tend only to achieve the desired nearfield beampattern over a limited range of angles because they focus the array to a single point in three dimensional space. Other methods that deal explicitly with nearfield beamforming include [5]–[7].

We use a nearfield-farfield transformation [8] as a theoretical tool to establish the asymptotic equivalence up to complex conjugation of two transformation problems: 1) determining the nearfield performance of a desired beampattern specification in the farfield and 2) determining the equivalent farfield beampattern corresponding to a given desired beampattern specification in the nearfield. As a consequence of this relationship, we show that the computationally difficult nearfield-farfield transformation [8] may be circumvented by use of a simpler farfield to nearfield determination. Equally importantly, we show that farfield techniques may be used directly to solve the nearfield beamformer design problem. This design process is independent of the wave equation based decompositions that lie at the heart of some design procedures such as those given in [8].

The paper is organized as follows. The following section describes how a beampattern specification may be represented as an orthogonal expansion in spherical coordinates. Section III derives a relationship between a beampattern specification at one radius and a beampattern specification at a second radius. Based on this relationship, Section IV outlines a novel computationally simple nearfield beamformer design technique based on the nearfield-farfield reciprocity relationship. Finally, a simulation example is presented in Section V and the paper is concluded in Section VI.

II. Beampattern Formulation

At the physical level, beamforming is characterized by the wave equation. In the engineering literature, this detail of modeling is usually unnecessary as much simpler formulations can be made exploiting the common array geometries (typically equally spaced sensors in a straight line), phasor representations (where the time dependence through the frequency of modulation is not explicitly indicated), and farfield data (facilitating the use of the Fourier Transform). The modal decomposition of the solution to the wave equation presents a preferred way to represent a beampattern as a sum of appropriately weighted orthogonal functions of the spatial coordinates. When represented in spherical coordinates, this decomposition lends two advantages: The beampattern can be readily determined at any radial distance (not just at infinity), and the radial dependence enters in a separable fashion that is independent of direction (azimuth and elevation).

Manuscript received September 24, 1996; revised June 5, 1998. The associate editor coordinating the review of this paper and approving it for publication was Dr. Ananthram Swami.

R. A. Kennedy is with the Telecommunications Engineering Group, RSISE, Australian National University, Canberra, Australia.

D. B. Ward is with the School of Electrical Engineering, University College (UNSW), Australian Defence Force Academy, Canberra, Australia.

T. D. Abhayapala is with the Telecommunication Engineering Group, Research School of Information Sciences and Engineering, Australian National University, Canberra, Australia.

Publisher Item Identifier S 1053-587X(99)00168-3.

[1] One such example is speech acquisition with a microphone array, which finds application in teleconferencing, hands-free telephones, and voice-only data entry (see, e.g., [2]–[4]).

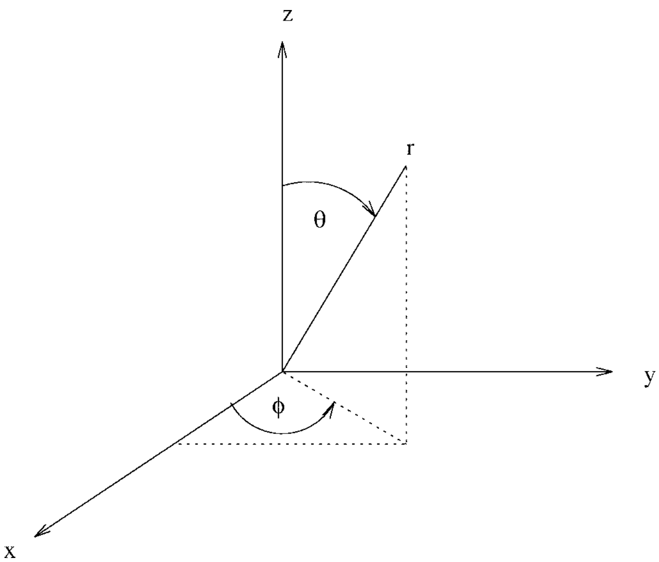

Fig. 1. Spherical coordinate system.

Let r denote radial distance, and let ϕ and θ denote the azimuth and elevation angles, respectively, as shown in Fig. 1. Then, a general solution to the classical wave equation in the *beampattern* form (synthesis equation) under mild condition [8] is given by

$$b_r(\theta, \phi) = \sum_{n=0}^{\infty} \sum_{m=-n}^{n} \alpha_n^m r^{\frac{1}{2}} H_{n+\frac{1}{2}}^{(1)}(kr) P_n^{|m|}(\cos\theta) e^{jm\phi} \quad (1)$$

where m and n are integers, $k \triangleq 2\pi f/c = 2\pi/\lambda$ is the wavenumber that can be expressed in terms of the propagation speed c and the frequency f or the wavelength λ, $P_n^m(\cdot)$ is the associated Legendre function, and $H_{n+\frac{1}{2}}^{(1)}(\cdot)$ is the half odd integer order Hankel Function of the first kind. The Fourier-like complex constants α_n^m can be expressed explicitly (analysis equation) as

$$\alpha_n^m = \frac{\zeta_n^m \mathcal{A}_{mn}(b)}{r_b^{\frac{1}{2}} H_{n+\frac{1}{2}}^{(1)}(kr_b)} \quad (2)$$

where r_b is the radius corresponding to the $b \equiv b(\theta, \phi)$ specification

$$\mathcal{A}_{mn}(b) \triangleq \zeta_n^m \int_0^{2\pi}\int_0^{\pi} b(\theta,\phi) P_n^{|m|}(\cos\theta) \sin\theta e^{-jm\phi}\, d\theta\, d\phi \quad (3)$$

and

$$\zeta_n^m \triangleq \sqrt{\frac{2n+1}{4\pi}\frac{(n-|m|)!}{(n+|m|)!}}.$$

Based on the above results, we can make two observations:

1) Since the complex coefficients (2), in the expansion (1), completely characterize the beampattern at all distances, the beampattern response can be reconstructed at arbitrary points in space.
2) There is a significant computational burden in accurately evaluating the coefficients (2) because of the multidimensional integration necessary from (3). Overcoming this complication is the major motivation for the development of our novel scheme.

III. Radial Transformations and Reciprocity

A. Problem Formulation

The objective is to relate a beampattern specification given on a sphere at one radius, say, r_1 from the origin, to a beampattern specification at a second radius, say, r_2 from the origin. This is achieved by beampattern analysis at r_1 [through (2)] and resynthesis at r_2 [through (1)]. The key technical observation we make is that this problem is essentially identical to the problem of beampattern analysis at r_2 and resynthesis at r_1 (for a different solution to the wave equation) up to complex conjugation and an error term that is typically small for problems of interest. This is exploited later in a nearfield design procedure given in Section IV-B, which permits bypassing the computationally difficult analysis step of the exact design method [8], which we characterize.

B. Asymptotic Equivalence

Given that our key technical development is cast in terms of asymptotic equivalence, we present some concise definitions.

Let $g(x)$ and $f(x)$ be two complex functions of a real variable x within some real domain $\mathcal{D}$ both possessing limits as $x \to x_0$ in $\mathcal{D}$; then, we say that $f(x) = O(g(x))$ as $x \to x_0$ if there exists positive constants K and δ such that $|f| \le K|g|$ whenever $0 < |x - x_0| < \delta$.

We say that $f(x)$ is *asymptotically equivalent* to $g(x)$ under the limit $x \to x_0$ if f and g are such that $\lim_{x\to x_0} f/g = 1$. The notation in this case is $f(x) \sim g(x)$ as $x \to x_0$. As an example of asymptotic equivalence, we can write

$$H_{n+\frac{1}{2}}^{(1)}(kr) \sim (-j)^{n+1}\sqrt{\frac{2}{\pi kr}} e^{jkr} \quad \text{as } r \to \infty \quad (4)$$

which follows from (19) in the Appendix.

C. Hankel Function Property

Associated with a single mode indexed by n (and independent of m), we have a reciprocity relationship, which is given next. It is referred to as a reciprocity relationship because the radial behavior relating an ordered pair of distances (r_1, r_2) for one beampattern problem can be related to the reversed ordered pair (r_2, r_1) of another beampattern problem after complex conjugation and up to some error term related to the closeness of r_1 and r_2.

Proposition 1: Let $H_{n+\frac{1}{2}}^{(1)}(\cdot)$ and $H_{n+\frac{1}{2}}^{(2)}(\cdot)$ denote the half odd integer order Hankel functions of the first and second kinds, respectively, where

n	modal index;
λ	wavelength;
$k = 2\pi/\lambda$	wavenumber.

Then

$$\frac{r_1^{\frac{1}{2}} H^{(1)}_{n+\frac{1}{2}}(kr_1)}{r_2^{\frac{1}{2}} H^{(1)}_{n+\frac{1}{2}}(kr_2)} = \frac{r_2^{\frac{1}{2}} H^{(2)}_{n+\frac{1}{2}}(kr_2)}{r_1^{\frac{1}{2}} H^{(2)}_{n+\frac{1}{2}}(kr_1)}(1+\epsilon(n,kr_1,kr_2)) \quad \text{(5a)}$$

where

$$\epsilon(n,kr_1,kr_2) = \frac{n(n+1)}{2k^2}\left(\frac{1}{r_2^2} - \frac{1}{r_1^2}\right) + O\left(\frac{1}{k^4 r^4}\right) \quad \text{as } r\to\infty \quad \text{(5b)}$$

with $r = \min(r_1, r_2)$.

The proof of Proposition 1 is given in the Appendix. We make the following observations regarding this result. We can take $r_1 = r < \infty$ and $r_2 = \infty$ to make the reciprocity between the nearfield and the farfield. The quantities in (5a) are complex. However, the error $\epsilon(n, kr_1, kr_2)$ term is purely real, meaning the error is only in the magnitude, or equivalently, there is no error in the phase angle. This follows from the property $\arg(z_1/z_2) = \arg(z_2^*/z_1^*)$, where z_1 and z_2 are complex numbers.

D. Key Reciprocity Relationship

We now show how beampattern specification (analysis) at r_1 and resynthesis at r_2 relates to a conjugate beampattern specification (analysis) at r_2 and resynthesis at r_1, leading to Proposition 2 below. While modal techniques are used to evaluate the result, they are not needed to use the result.

With a beampattern $b(\theta,\phi)$ specification given at radius r_1, the resultant beampattern at distance r_2 is denoted and given by

$$b_{r_2}(\theta,\phi)\big|_{b_{r_1}=b} = \sum_{n=0}^{\infty} \frac{r_2^{\frac{1}{2}} H^{(1)}_{n+\frac{1}{2}}(kr_2)}{r_1^{\frac{1}{2}} H^{(1)}_{n+\frac{1}{2}}(kr_1)} \times \sum_{m=-n}^{n} \zeta_n^m \mathcal{A}_{mn}(b) P_n^{|m|}(\cos\theta) e^{jm\phi}. \quad (6)$$

This equation follows from substituting (2) in (1).

Compare this with a complex conjugate beampattern $b^*(\theta,\phi)$ specification at radius r_2 that at r_1 results in

$$b_{r_1}(\theta,\phi)\big|_{b_{r_2}=b^*} = \sum_{n=0}^{\infty} \frac{r_1^{\frac{1}{2}} H^{(1)}_{n+\frac{1}{2}}(kr_1)}{r_2^{\frac{1}{2}} H^{(1)}_{n+\frac{1}{2}}(kr_2)} \times \sum_{m=-n}^{n} \zeta_n^m \mathcal{A}_{mn}(b^*) P_n^{|m|}(\cos\theta) e^{jm\phi}. \quad (7)$$

From (3), $\mathcal{A}_{mn}(b^*) = A^*_{(-m)n}(b)$. Then, taking the complex conjugate of (7) by change of variable m in the summation by $-m$ and then using Proposition 1 yields

$$b^*_{r_1}(\theta,\phi)\big|_{b_{r_2}=b^*} = \sum_{n=0}^{\infty} \frac{r_1^{\frac{1}{2}} H^{(2)}_{n+\frac{1}{2}}(kr_1)}{r_2^{\frac{1}{2}} H^{(2)}_{n+\frac{1}{2}}(kr_2)} \times \sum_{m=-n}^{n} \zeta_n^m \mathcal{A}_{mn}(b) P_n^{|m|}(\cos\theta) e^{jm\phi} = b_{r_2}(\theta,\phi)\big|_{b_{r_1}=b}\left(1 + O\left(\frac{1}{k^2 r_2^2} - \frac{1}{k^2 r_1^2}\right)\right) \quad (8)$$

as $r\to\infty$, where $r = \min(r_1, r_2)$ (alternatively, for $r_1 \to r_2$, this also holds). Thus, we have established the following proposition.

Proposition 2: Let λ be the wavelength and $k = 2\pi/\lambda$ the wave number; then

$$b^*_{r_1}(\theta,\phi)\big|_{b_{r_2}=b^*} = b_{r_2}(\theta,\phi)\big|_{b_{r_1}=b}\left(1 + O\left(\frac{1}{k^2 r_2^2} - \frac{1}{k^2 r_1^2}\right)\right) \quad (9)$$

as $r\to\infty$, where $r = \min(r_1, r_2)$.

By associating r_1 with the nearfield and r_2 with the farfield, this proposition establishes an asymptotic equivalence, up to complex conjugation, of two problems: 1) determining the nearfield performance of a farfield beampattern specification and 2) determining the equivalent farfield beampattern corresponding to a nearfield beampattern specification. We make the following observations.

1) If $r_2 = \infty$, then this result is saying that a nearfield problem can be solved approximately by solving a related farfield problem.
2) Consider the tradeoff between operating at a distance (measured in wavelengths) sufficiently large to ensure the dominant error term in (5b) to be small. (For analysis purposes, we take $r_1 = r$ and $r_2 = \infty$.) This requires, after taking the square root

$$\sqrt{\frac{n(n+1)}{8\pi^2}} \ll \frac{r}{\lambda} \quad (10)$$

whereas for the first-order term in the asymptotic expansion of $H^{(1)}_{n+\frac{1}{2}}(kr)$ (4) to be small [see (19) in the Appendix] requires

$$\frac{n(n+1)}{4\pi} \ll \frac{r}{\lambda}. \quad (11)$$

This shows the asymptotic reciprocity holds much better than might be gleaned by taking a naive approach of operating at a distance with r/λ large enough such to guarantee the asymptotic form (4) can be used as an approximation. Further, the true dominant error term (10) grows linearly with n relative to r/λ versus the naive condition (11), which grows quadratically with n relative to r/λ.
3) The reciprocity holds whenever the dominant error term can be made small, which implies either the beampattern is lowpass in character, i.e., most of the energy is in the lower order modes (small n, which generally holds), or the difference in the radial distances $r_1 - r_2$ is small enough. The meaning of the former condition will be fleshed out later in Section V-C.

IV. Nearfield Design Procedures

A. Background

A largely hitherto unrecognized fact in the signal processing literature before [8] is that any nearfield beampattern specification can be transformed into an equivalent farfield specification. That is, realizing through design, a particular well-defined farfield beampattern specification achieves, without approximation, a desired nearfield beampattern specification.

In this work, we restrict attention to a nearfield specification on a sphere that simplifies the analysis equations. However, the result can be generalized to a nearfield beampattern specification on an arbitrary manifold at the cost of further complication in determining α_n^m in (1).

An exact nearfield design [8] can be implemented by transforming the nearfield specification $b(\theta,\phi)$ defined on a sphere of radius r to the farfield. This method requires in the analysis step (3) multidimensional numerical integrations to be performed, which must contend with numerical issues. The advantage of the radial reciprocity technique defined in Section IV-B, although only asymptotically exact, is that *no analysis step or modal expansion needs to be performed*. This leads to a sequence of computationally straightforward signal processing steps to achieve a high-quality nearfield design.

B. Novel Design Using Reciprocity

The reciprocity relationship (9) with $r_1 = r$ and $r_2 = \infty$ leads to the corollary of Proposition 2.

Proposition 3: The farfield beampattern corresponding to a desired nearfield beampattern specification $b_r(\theta,\phi) = b(\theta,\phi)$ satisfies the asymptotic equivalence

$$b_\infty(\theta,\phi)\big|_{b_r=b} \sim b_r^*(\theta,\phi)\big|_{b_\infty=b^*}, \quad \text{as } r\to\infty. \tag{12}$$

By assuming (12) holds with equality, we have the following approximate design procedure.

Nearfield Design Procedure

- Step 0) Specify the desired nearfield beampattern $b(\theta,\phi)$ at distance r.
- Step 1) Synthesize the farfield beampattern $b^*(\theta,\phi)$ at $r_2=\infty$, i.e., $b_\infty(\theta,\phi) = b^*(\theta,\phi)$.
- Step 2) Using the sensor weights of Step 1) evaluate the resultant nearfield beampattern $a(\theta,\phi)$ at r, i.e., $a(\theta,\phi) = b_r(\theta,\phi)\big|_{b_\infty=b^*}$.
- Step 3) Synthesize a farfield beampattern $a^*(\theta,\phi)$ at $r_2 = \infty$. These weights will produce the desired beampattern $b(\theta,\phi)$ at distance r.

This procedure requires a nearfield beampattern determination from farfield data sandwiched between two farfield designs.

The farfield design in Step 1 may be implemented as follows. Determine N sensor weights $\{w_n\}$ using standard farfield techniques to synthesize the response using

$$b^*(\theta,\phi) = \sum_{n=0}^{N-1} w_n e^{jk(x_n\sin\theta\cos\phi + y_n\sin\theta\sin\phi + z_n\cos\theta)} \tag{13}$$

where (x_n, y_n, z_n) is the location of the nth sensor—this is a well-studied design procedure and can be effected by using least squares techniques.

Step 2) requires determination of the nearfield response from the farfield design. The response can be computed using the weights and array geometry used in Step 1), i.e.,

$$a(\theta,\phi) = C\sum_{n=0}^{N-1} w_n \frac{e^{jkd_n(r,\theta,\phi)}}{d_n(r,\theta,\phi)} \tag{14}$$

where $d_n(r,\theta,\phi)$ is the distance from a point at (r,θ,ϕ) to the nth sensor, and C is some normalizing complex constant. Note that in (14), we use the propagation model where magnitude attenuates like the reciprocal of distance and the phase is proportional to distance. This type of response determination [see (14)], which requires explicit sensor locations and weights, can be contrasted with the more general methods given in Section III-D and [8], which do not require any array geometry information [but do require the determination of the modal weights (3)].

The final step [Step 3)] determines the $\tilde{N}$ sensor weights $\tilde{w}_n$ to give the farfield response

$$a^*(\theta,\phi) = \sum_{n=0}^{\tilde{N}-1} \tilde{w}_n e^{jk(\tilde{x}_n\sin\theta\cos\phi + \tilde{y}_n\sin\theta\sin\phi + \tilde{z}_n\cos\theta)} \tag{15}$$

where $(\tilde{x}_n, \tilde{y}_n, \tilde{z}_n)$ is the location of the nth sensor. Note that this array geometry need not necessarily be the same as in Step 1 but should correspond to the actual array. A typical design procedure is illustrated in the next section.

The primary utility in the procedure is the circumvention of the computationally nontrivial transformation from a desired nearfield beampattern to the equivalent farfield beampattern requiring numerical integration and the direct use of farfield design procedures.

V. Design Example and Analysis

A. Parseval Relation

Here, we present a Parseval relation, which will be essential later in assessing the novel design using reciprocity by determining the distribution of power across the modal components for a given beampattern specification on a sphere of arbitrary radius.

The beampattern form of the wave equation $b_r(\theta,\phi)$ in (1) gives the field strength in an incremental solid angle $\sin\theta\, d\theta\, d\phi$ on a sphere of radius r, leading to the following Parseval relation.

Proposition 4: Let $b_r(\theta,\phi) = b(\theta,\phi)$ be the beampattern specification (at radius r). Then

$$\int_0^{2\pi}\int_0^{\pi} |b_r(\theta,\phi)|^2 \sin\theta\, d\theta\, d\phi = \sum_{n=0}^{\infty}\sum_{m=-n}^{n} |\mathcal{A}_{mn}(b)|^2 \tag{16}$$

where $b \equiv b(\theta,\phi)$, and $\mathcal{A}_{mn}(b)$ is given by (3).

The proof is given in the Appendix.

An observation regarding the $\mathcal{A}_{mn}(b)$ in (3) is that these represent modal amplitudes and depend only on the shape of the beampattern and not on the radius of the sphere on which the beampattern is given, e.g., the computation is identical whether the beampattern is nearfield or farfield.

The Parseval relation (16) gives some engineering insights into the number of modes with significant power required to get a good beampattern match. In close analogy with frequency domain filter analysis, we will see that the lower order modes are the significant ones that give the broad beampattern features (analogous to the lower frequencies in a filter design problem), whereas the higher order modes give the finer detail (analogous to higher frequencies in a filter design

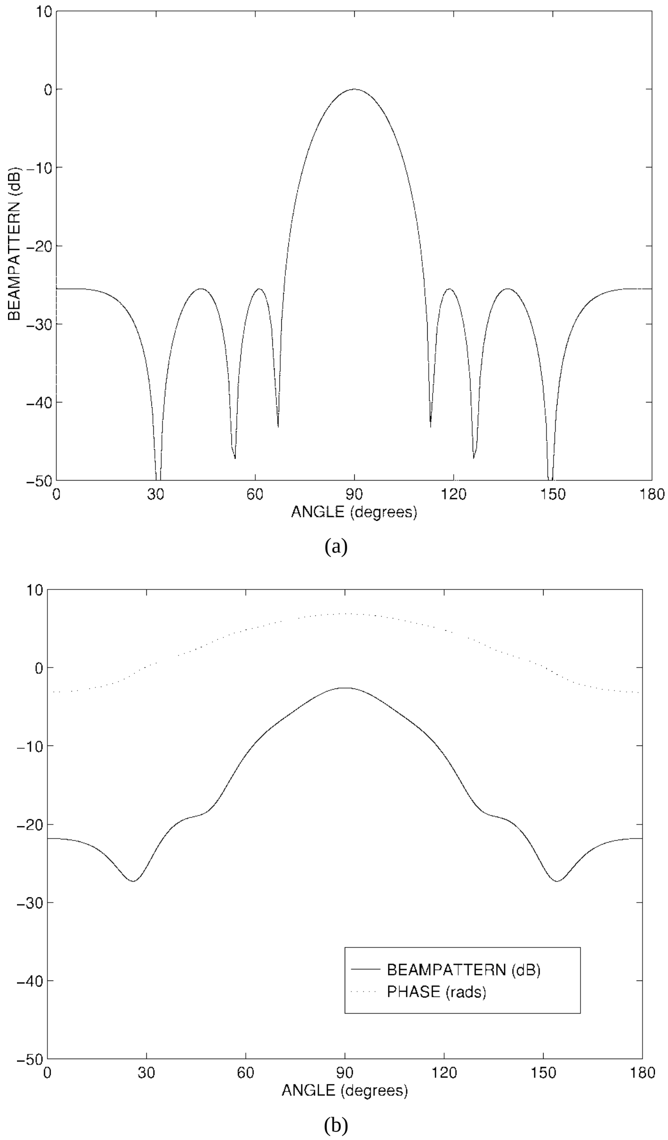

Fig. 2. Demonstration of Steps 0, 1, and 2 of the nearfield design procedure using nearfield/farfield reciprocity.

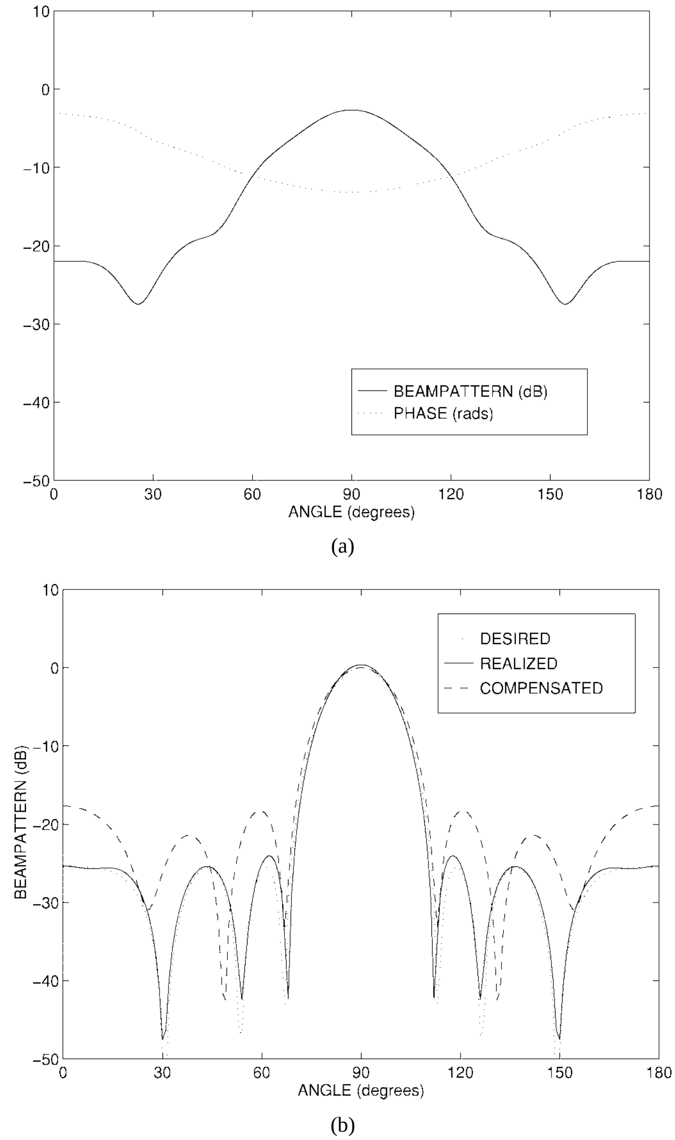

Fig. 3. Demonstration of Step 3 of the nearfield design procedure using nearfield/farfield reciprocity.

problem). We assert that sensible beampattern specifications should involve only the lower order modes. As indicated in the following example, whenever such a "lowpass" beampattern specification is used, the novel design procedure using reciprocity has been observed to work extremely well. The analysis that follows the example puts substance to these claims.

B. Linear 1-D Array Example

The following example shows the result of the nearfield design procedure of Section IV-B in comparison with a technique developed in [4]. The objective was to realize a seventh-order zero-phase Chebyshev 25-dB beampattern, which is shown in Fig. 2(a), in the nearfield at a radius of three wavelengths—this is Step 0) of the nearfield design procedure. The array sensors are colinear and aligned along the z axis in Fig. 1.

Step 1) of the nearfield design procedure required a design to realize the complex conjugate of this Chebyshev beampattern in the farfield. This is a classical design problem [9], and the weights for a seven-sensor half-wavelength spaced farfield array are easily calculated. The resultant designed farfield beampattern is identical to that shown in Fig. 2(a). This is $b^*(\theta, \phi)$ in the design procedure, i.e., the complex conjugate of the objective beampattern.

The response of this farfield beamformer was then evaluated in the nearfield at the required radius of three wavelengths according to (14). Fig. 2(b) shows the resulting beampattern. This is $a(\theta, \phi)$ in Step 2) of the nearfield design procedure.

Step 3) of the nearfield design procedure required designing a farfield beamformer to realize $a^*(\theta, \phi)$. We used a weighted complex-valued least-squares design method [10] to realize $a^*(\theta, \phi)$ with a quarter-wavelength spaced array. Thirteen elements, corresponding to a three-wavelength aperture, were used to achieve an adequate match to the desired beampattern. Angles outside the range 70°–110° were weighted more heavily so that the sidelobe region of the desired Chebyshev beampattern would be accurately approximated. The resulting farfield realization is shown in Fig. 3(a).

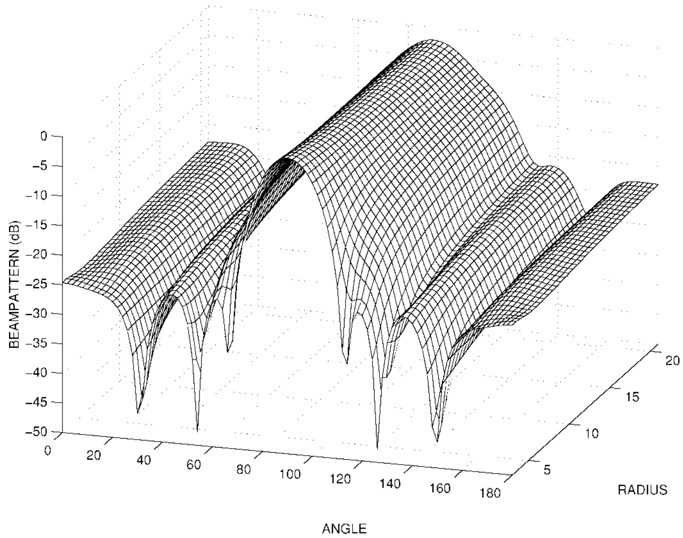

Fig. 4. Performance of the beamformer design magnitude as a function of angle(degrees) and radial distance (wavelengths). The phase response is not shown.

Finally, to verify that the design objectives had been met, this beamformer was simulated in the nearfield at a radius of three wavelengths; the nearfield beampattern shown solid in Fig. 3(b) resulted. The desired Chebyshev 25 dB beampattern (dotted) is also shown, as is the response of the nearfield method of [4] (dashed). We note that the proposed nearfield design technique provides a very close realization of the desired beampattern over all angles and not just at angles close to broadside as for the nearfield method of [4]. Fig. 4 shows the performance of the beamformer versus angle (degrees) and distance (wavelengths). It shows the desired beampattern at three wavelengths (near edge) and the variation with distance as we move toward the farfield (far edge).

This example highlights the main feature of our proposed nearfield beamforming procedure. When the reciprocity relation holds, it is only necessary to use well-established farfield beamformer design techniques in the design of a nearfield beamformer.

C. Modal Analysis of the Example

Since the array sensors are aligned along the z axis only, the $m = 0$ modes are potentially nonzero, i.e., only the $\mathcal{A}_n^0(b)$ coefficients [see (3)] can be nonzero. Further, since the phase is zero for this example, the $\mathcal{A}_n^0(b)$ coefficients are purely real, and because the beampattern is symmetric, the odd coefficients are zero.

In order to determine the validity of the reciprocity relation (9), we analyze the modal expansion for this example. The results are summarized in Table I and Fig. 5. Table I shows a decomposition of the beampattern as a modal expansion indexed by n.

A conservative check can first be made by seeing whether (10) is satisfied for all significant terms used in the beampattern synthesis equation (1). The Parseval relation (16) identifies the power contained in each $(m = 0)$ mode with $|\mathcal{A}_n^0(b)|^2$. In this way, we can see the error measured in beampattern power

TABLE I
POWER AND ERRORS VERSUS MODAL COEFFICIENTS FOR EXAMPLE 1

n	$\mathcal{A}_n^0(b)$	$\lvert\epsilon(n, 6\pi, \infty)\rvert$	$\lvert\mathcal{A}_n^0(b)\rvert^2$	% Pow	% Err
0	0.748830	0.000000	0.560746	27.7	0.0
2	-0.790121	0.008443	0.624291	30.8	0.3
4	0.619535	0.028145	0.383824	18.9	0.5
6	-0.560184	0.059104	0.313806	15.5	0.9
8	0.353918	0.101321	0.125258	6.2	0.6
10	-0.129829	0.154796	0.016855	0.8	0.1
12	0.029584	0.219529	0.000875	0.0	0.0
14	-0.004547	0.295520	0.000021	0.0	0.0
16	0.000504	0.382769	0.000000	0.0	0.0
18	-0.000042	0.481276	0.000000	0.0	0.0
20	0.000003	0.591040	0.000000	0.0	0.0
22	0.000000	0.712063	0.000000	0.0	0.0
24	0.000000	0.844343	0.000000	0.0	0.0
Sum	n/a	n/a	2.025676	100.0	2.5

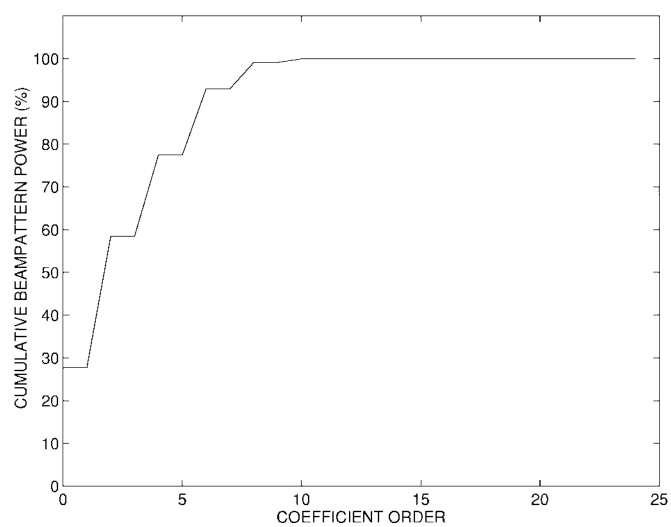

Fig. 5. Number of terms required in (1) to accurately model a seventh-order Chebyshev 25 dB beampattern. There is insignificant power beyond the tenth order mode.

associated with using a finite number of analysis coefficients in the synthesis equation (1); in addition, we see which are the dominant modes. Using this Parseval expression, we calculated the power in each mode in the fourth column of Table I. In Fig. 5, we have plotted the cumulative beampattern power versus n. Clearly, only the even terms up to $n = 10$ are significant. Substituting $n = 10$ into the error bound (10) gives

$$\frac{\sqrt{55}}{2\pi} \approx 1.068 \ll \frac{r}{\lambda}$$

which can be compared with our design for $r = 3$ wavelengths. Note that for this distance $kr = 6\pi$, and we take $r_1 = r$ and $r_2 = \infty$.

A more detailed examination of the modal expansion shows that the lower order modes (small n) dominant the power, but it is these modes that contribute the least asymptotic error in (5). From (5), for the parameters in this example, we have

$$|\epsilon(n, 6\pi, \infty)| = \frac{n(n+1)}{72\pi^2} \tag{17}$$

which is computed in the third column of Table I. However, to better gauge the overall error this causes to the reciprocity condition (9), we weight these error magnitudes by the power in the corresponding mode, and the result is the sixth column of Table I, which is provided as a guide only. Therefore, it can be seen that an upper bound on the approximate accuracy of the reciprocity is, at most, of the order of 2.5% in error.

VI. Summary

Nearfield modal beamforming (based on the wave equation) can lead to an approximation-free design formulation—nearfield beampattern specifications can be transformed to a strictly equivalent farfield beampattern, liberating a plethora of farfield design techniques to tackle nearfield design problems. This paper identifies that the computation of the modal representation represents a hurdle in fully exploiting this design strategy and presents a novel computationally straightforward design procedure that asymptotically achieves the same goal without recourse to a modal decomposition.

Appendix
Proofs of Key Technical Results

Proof of Proposition 1: Since $H^{(2)}_{n+\frac{1}{2}}(\cdot)$ is the complex conjugate of $H^{(1)}_{n+\frac{1}{2}}(\cdot)$, it is sufficient to characterize the behavior of $H^{(1)}_{n+\frac{1}{2}}(\cdot)$, which may be defined through the recursion

$$H^{(1)}_{n+\frac{3}{2}}(x) = \frac{(2n+1)}{x} H^{(1)}_{n+\frac{1}{2}}(x) - H^{(1)}_{n-\frac{1}{2}}(x) \tag{18}$$

with

$$H^{(1)}_{\frac{1}{2}}(x) = -jH^{(1)}_{-\frac{1}{2}}(x) = -j\sqrt{\frac{2}{\pi x}}e^{jx}.$$

From the form of the recursion [see (18)] and after some simplification, it follows that

$$H^{(1)}_{n+\frac{1}{2}}(x) = (-j)^{n+1} \underbrace{\left(1 + \sum_{i=1}^{n} \frac{\xi_{i,n}}{(-jx)^i}\right)}_{p_n(-jx)} \sqrt{\frac{2}{\pi x}} e^{jx}$$

for some n real-valued coefficients $\xi_{i,n}$. These coefficients can be readily determined in the form

$$p_n(z) = 1 + \sum_{i=1}^{n} \frac{1}{2^i i!} \frac{(n+i)!}{(n-i)!} \frac{1}{z^i}$$

leading to the asymptotic representation

$$\begin{aligned} H^{(1)}_{n+\frac{1}{2}}(x) = (-j)^{n+1} \Bigg(1 + j\frac{1}{2x} n(n+1) - \frac{1}{8x^2}\frac{(n+2)!}{(n-2)!} \\ + O\left(\frac{1}{x^3}\right)\Bigg)\sqrt{\frac{2}{\pi x}} e^{jx} \end{aligned} \tag{19}$$

as $x \to \infty$.

Of interest in proving the proposition is the square magnitude of the polynomial portion of the Hankel function, which can be written

$$\begin{aligned} \left|1 + \sum_{i=1}^{n} \frac{\xi_{i,n}}{(-jx)^i}\right|^2 &\triangleq 1 + \sum_{i=1}^{n} \frac{\eta_{i,n}}{x^{2i}} \\ &= 1 + \underbrace{\left(\xi_{1,n}^2 - 2\xi_{2,n}\right)}_{\eta_{1,n}} \frac{1}{x^2} \\ &\quad + \underbrace{\left(\xi_{2,n}^2 + 2\xi_{4,n} - 2\xi_{1,n}\xi_{3,n}\right)}_{\eta_{2,n}} \frac{1}{x^4} + O\left(\frac{1}{x^6}\right) \end{aligned}$$

where $\eta_{i,n}$ are suitable real-valued coefficients. From (5a)

$$\begin{aligned} 1 + \epsilon(n, x_1, x_2) &= \left|x_1^{\frac{1}{2}} H^{(1)}_{n+\frac{1}{2}}(x_1)\right|^2 \Big/ \left|x_2^{\frac{1}{2}} H^{(1)}_{n+\frac{1}{2}}(x_2)\right|^2 \\ &= \left(1 + \frac{\eta_{1,n}}{x_1^2} + \frac{\eta_{2,n}}{x_1^4} + O\left(\frac{1}{x_1^6}\right)\right) \Bigg/ \\ &\quad \left(1 + \frac{\eta_{1,n}}{x_2^2} + \frac{\eta_{2,n}}{x_2^4} + O\left(\frac{1}{x_2^6}\right)\right) \\ &= \left(1 + \frac{\eta_{1,n}}{x_1^2} + \frac{\eta_{2,n}}{x_1^4} + O\left(\frac{1}{x_1^6}\right)\right) \\ &\quad \times \left(1 - \frac{\eta_{1,n}}{x_2^2} - \frac{\eta_{2,n}}{x_2^4} + \frac{\eta_{1,n}^2}{x_2^4} + O\left(\frac{1}{x_2^6}\right)\right) \\ &= 1 + \eta_{1,n}\left(\frac{1}{x_1^2} - \frac{1}{x_2^2}\right) + \eta_{2,n}\left(\frac{1}{x_1^4} - \frac{1}{x_2^4}\right) \\ &\quad + \eta_{1,n}^2 \frac{1}{x_2^2}\left(\frac{1}{x_2^2} - \frac{1}{x_1^2}\right) + O\left(\frac{1}{x^6}\right) \end{aligned}$$

as $x \to \infty$, where $x = \min(x_1, x_2)$. Using (19), the first correction term has coefficient

$$\eta_{1,n} = \xi_{1,n}^2 - 2\xi_{2,n} = \frac{1}{2}n(n+1).$$

Letting $x_1 = kr_1$ and $x_2 = kr_2$ establishes the result.

Proof of Proposition 4: Using (2) and (3), the beampattern synthesis equation (1) can be written

$$b_r(\theta, \phi) = \sum_{n=0}^{\infty} \sum_{m=-n}^{n} \zeta_n^m \mathcal{A}_{mn}(b) P_n^{|m|}(\cos\theta) e^{jm\phi} \tag{20}$$

when $r_b = r$. In the following, we simplify the notation by dropping explicit reference to the beampattern $b \equiv b(\theta, \phi)$, which is understood. With the change of variables $u = \cos\theta$, multiplying (20) by its complex conjugate, and integrating with respect to θ and ϕ gives

$$\int_0^{2\pi}\int_0^{\pi} |b_r(\theta,\phi)|^2 \sin\theta\, d\theta\, d\phi = \int_0^{2\pi}\int_{-1}^{1} |b_r(u,\phi)|^2\, du\, d\phi = \Lambda$$

where

$$\Lambda \triangleq \sum_{n=0}^{\infty}\sum_{m=-n}^{n}\sum_{k=0}^{\infty}\sum_{l=-k}^{k} \zeta_n^m \zeta_k^l \left(\int_{-1}^{1} P_n^{|m|}(u) P_k^{|l|}(u)\, du\right) \times \left(\int_0^{2\pi} \mathcal{A}_{mn}\mathcal{A}_{lk}{}^{*} e^{j(m-l)\phi}\, d\phi\right).$$

The orthogonality property of the associated Legendre function [11] is

$$2\pi \int_{-1}^{1} P_n^m(u) P_k^m(u)\, du = \begin{cases} 0, & n \neq k \\ (\zeta_n^m)^{-2}, & n = k. \end{cases} \tag{21}$$

By substituting (21) and carrying out the integration with respect to ϕ gives

$$\Lambda = \sum_{n=0}^{\infty}\sum_{m=-n}^{n} |\mathcal{A}_{mn}|^2.$$

References

[1] R. J. Mailloux, *Phased Array Antenna Handbook*. Boston, MA: Artech House, 1994.
[2] J. L. Flanagan, D. A. Berkeley, G. W. Elko, J. E. West, and M. M. Sondhi, "Autodirective microphone systems," *Acoustica*, vol. 73, pp. 58–71, 1991.
[3] Y. Grenier, "A microphone array for car environments," *Speech Commun.*, vol. 12, no. 1, pp. 25–39, Mar. 1993.
[4] F. Khalil, J. P. Jullien, and A. Gilloire, "Microphone array for sound pickup in teleconference systems," *J. Audio Eng. Soc.*, vol. 42, no. 9, pp. 691–700, Sept. 1994.
[5] S. Nordebo, I. Claesson, and S. Nordholm, "Weighted Chebyshev approximation for the design of broadband beamformers using quadratic programming," *IEEE Signal Processing Lett.*, vol. 1, pp. 103–105, July 1994.
[6] B. D. Carlson and D. Willner, "Antenna pattern synthesis using weighted least squares," *Proc. Inst. Elect. Eng. H, Microw., Opt. Antennas*, vol. 139, no. 1, pp. 11–16, Feb. 1992.
[7] M. F. Berger and H. F. Silverman, "Microphone array optimization by stochastic region contraction," *IEEE Trans. Signal Processing*, vol. 39, pp. 2377–2386, Nov. 1991.
[8] R. A. Kennedy, T. Abhayapala, and D. B. Ward, "Broadband nearfield beamforming using a radial beampattern transformation," *IEEE Trans. Signal Processing*, vol. 46, pp. 2147–2156, Aug. 1998.
[9] C. L. Dolph, "A current distribution for broadside arrays which optimizes the relationship between beam width and side-lobe level," *Proc. IRE*, vol. 34, pp. 335–348, June 1946.
[10] B. D. Van Veen and K. M. Buckley, "Beamforming: A versatile approach to spatial filtering," *IEEE Acoust., Speech, Signal Processing Mag.*, vol. 5, pp. 4–24, Apr. 1988.
[11] M. R. Spiegel, *Mathematical Handbook of Formulas and Tables*. New York: McGraw-Hill, 1968.

Rodney A. Kennedy (M'90) was born in Sydney, Australia, on October 23, 1960. He received the B.E. (Hons.) degree in electrical engineering from the University of New South Wales, Sydney, in 1982. He received the M.E. degree in digital control theory from the University of Newcastle, Newcastle, Australia, in 1986 and the Ph.D. degree in telecommunications from the Department of Systems Engineering, Australian National University, Canberra, in 1988.

From 1983 to 1985, he was a research engineer at CSIRO Division of Radiophysics, Sydney. Since 1994, he has been Head of Department of the Telecommunication Engineering Group, Research School of Information Sciences and Engineering, Australian National University. His research interests are in the fields of digital communications and signal processing.

Dr. Kennedy is currently an Associate Editor for Data Communications for the IEEE TRANSACTIONS ON COMMUNICATIONS.

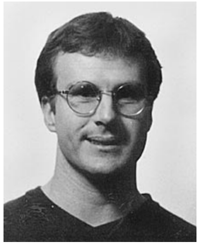

Darren B. Ward was born in Mareeba, Australia, on September 12, 1970. He received the B.E. (Hons.) degree in electronic engineering and the B.A.S. degree in computer science from the Queensland University of Technology, Brisbane, Australia, in 1992, and the Ph.D. degree from the Department of Engineering, Australian National University, Canberra, in 1996.

From December 1996 to June 1998, he was a Postdoctoral Member of Technical Staff in the Acoustics and Speech Research Department, Bell Laboratories Lucent Technologies, Murray Hill, NJ. Currently, he is a Lecturer with the School of Electrical Engineering, University College (UNSW), Australian Defence Force Academy, Canberra. His research interests include signal processing, digital communications, and electroacoustics.

Thushara D. Abhayapala (S'96) was born in Colombo, Sri Lanka, on March 1, 1967. He received the B.E. (Hons.) degree in interdisciplinary systems engineering from the Australian National University, Canberra, in 1994. He is currently pursuing the Ph.D. degree at the Telecommunication Engineering Group, Research School of Information Sciences and Engineering, Australian National University.

From 1995 to 1997, he was employed as a Research Engineer at the Arthur C. Clarke Centre for Modern Technologies, Katubedda, Moratuwa, Sri Lanka. His research interest are in the areas of array processing and multi-dimensional signal processing.